Excitation functions for production of Rf isotopes in the ^{248}Cm + ^{18}O reaction

M. Murakami,* S. Goto, H. Murayama, T. Kojima, and H. Kudo†
Department of Chemistry, Niigata University, Niigata, Niigata 950-2181, Japan

D. Kaji, K. Morimoto, H. Haba, Y. Kudou, T. Sumita, R. Sakai, A. Yoneda, and K. Morita
Nishina Center for Accelerator-Based Science, RIKEN, Wako, Saitama 351-0198, Japan

Y. Kasamatsu
Graduate School of Science, Osaka University, Toyonaka, Osaka 560-0043, Japan

H. Kikunaga
Research Center for Electron Photon Science, Tohoku University, Sendai, Miyagi 982-0826, Japan

T. K. Sato
Advanced Science Research Center, Japan Atomic Energy Agency, Tokai, Ibaraki 319-1195, Japan
(Received 30 May 2013; published 30 August 2013)

Production cross sections of Rf isotopes in the ^{248}Cm + ^{18}O reaction were measured at the beam energy range of 88.2 to 101.3 MeV by use of a gas-filled recoil ion separator. The excitation functions of ^{260}Rf, ^{261}Rf^{a}, and ^{262}Rf were obtained together with those of spontaneously fissioning nuclides which have few-second half-lives and have been assigned to ^{261}Rf^{b} and a longer-lived state of ^{262}Rf. The excitation function of few-second spontaneously fissioning nuclide exhibited the maximum cross section at the ^{18}O beam energy of 94.8 MeV. The shape of the excitation function was almost the same as that of ^{261}Rf^{a}, whereas it was quite different from those of ^{260}Rf and ^{262}Rf. A few-second spontaneously fissioning nuclide previously reported as ^{261}Rf^{b} and ^{262}Rf observed in ^{248}Cm + ^{18}O reaction was identified as ^{261}Rf^{b}.

DOI: 10.1103/PhysRevC.88.024618 PACS number(s): 27.90.+b, 25.70.Jj, 23.35.+g, 25.85.Ca

I. INTRODUCTION

The nuclide ^{261}Rf has been used for chemical investigations of Rf [1–5] because it has a relatively long half-life of 68 s [6] and decays by emission of characteristic α particle with 8.28 MeV [7]. Rutherfordium-261 is usually produced in ^{248}Cm + ^{18}O and ^{244}Pu + ^{22}Ne reactions via 5n evaporation channel. In these reactions, a spontaneously fissioning nuclide with a few-second half-life had been also observed in addition to ^{261}Rf. In 1981, Hoffman *et al.* [8] reported that 1.5-s spontaneous fission (SF) activity observed in the bombardment of ^{248}Cm with 95-MeV ^{18}O seems to be ^{259}Fm based on the fission properties such as symmetric and narrow mass distribution and high total kinetic energy. In 1985, Somerville *et al.* [9] reported 47-ms SF activity in the same reaction in addition to 1.6-s SF activity. They assigned 47-ms SF activity to ^{262}Rf tentatively and the 1.6-s SF activity was left unassigned, unlike Hoffman *et al.* [8], because its cross section was much larger than that expected for ^{259}Fm. Lazarev *et al.* [10] reported in 1994 that they discovered ^{265}Sg and ^{266}Sg by the reaction of ^{248}Cm + ^{22}Ne and that the daughter nuclide of ^{266}Sg, ^{262}Rf, decayed by SF with a 1.2-s half-life. They regarded all α-SF correlation events as the results of the correlation of ^{266}Sg and ^{262}Rf. The reported half-life of 1.2 s for ^{262}Rf was quite different from 47 ms reported by Somerville *et al.* [9] and was similar to that of unassigned activity mentioned above. Later, in 1996, Lane *et al.* [11] interpreted that there are two states in ^{262}Rf and assumed that the nuclide with a few-second half-life in direct production of ^{262}Rf [8,9] was due to the mixture of ^{262}Rf and ^{259}Fm. Because 2.1-s SF activity was observed in the ^{244}Pu + ^{22}Ne reaction in which the production cross section of ^{259}Fm is very low, they ascribed this SF activity to the longer-lived state of ^{262}Rf. Thus, two SF states of ^{262}Rf with half-lives of 2.1 s and 47 ms are adopted in Ref. [12].

On the other hand, in the investigation of heavier nuclides such as ^{277}Cn [13–16] and ^{269}Hs [17,18], it became clear that their descendant ^{261}Rf decays with a few-second half-life either by SF or α-particle emission. The α-particle energy, 8.52 MeV, is markedly different from that of the known isotope of ^{261}Rf, 8.28 MeV. Because the decay properties of ^{261}Rf in the decay chains of ^{277}Cn were quite different from those of previously reported ones, Hofmann *et al.* [14] proposed there exist two states in ^{261}Rf. The existence of two isomeric states in both ^{261}Rf and ^{265}Sg were indicated by re-examination of the available ^{265,266}Sg decay events by Düllmann and Türler [19]. Very recently, Haba *et al.* [20] experimentally confirmed the decay pattern of two isomeric states in ^{265}Sg in addition to a few-second SF isomeric state in ^{261}Rf as a daughter nuclide of ^{265}Sg. They also observed 8.52 ± 0.05 MeV α branch of 1.9-s isomeric state in ^{261}Rf directly produced in the reaction of ^{248}Cm + ^{18}O [21]. Hereafter, two states in ^{261}Rf

*Present address: Nishina Center for Accelerator-Based Science, RIKEN, Wako, Saitama 351-0198, Japan; masashi.murakami@riken.jp
†hkudo@sc.niigata-u.ac.jp

are referred to as ^{261}Rf^{a} (half-life $T_{1/2} = 68$ s [6], α-particle energy $E_\alpha = 8.28$ MeV [7,21], SF branch $b_{\rm SF} < 0.11$ [22]) and ^{261}Rf^{b} ($T_{1/2} = 2.6$ s, $E_\alpha = 8.51$ MeV, $b_{\rm SF} = 0.82$ [20]) as denoted in Refs. [17–21].

Although SF nuclides with few-second half-lives reported as 1.2–4.7 s [10,16] have been assigned to both ^{261}Rf and ^{262}Rf, it is possible that these two SF nuclides are the same nuclide and one of these isomers is misassigned to the other. In this work, we measured the excitation functions of Rf isotopes produced in the ^{248}Cm + ^{18}O reaction to clarify the ambiguity on the assignment of a few-second SF nuclides.

II. EXPERIMENTAL

The experiments were performed at the RIKEN Heavy-Ion Linear Accelerator (RILAC) facility using a gas-filled recoil ion separator (GARIS). The experimental setup used in this work was similar to that described in Ref. [23].

A $^{248}Cm_2O_3$ target of 230 μg/cm^2 thickness was prepared by electrodeposition onto a 0.91-mg/cm^2 Ti backing foil. The isotopic composition of the Cm material used as the target was 0.022% ^{244}Cm, 0.130% ^{245}Cm, 3.169% ^{246}Cm, 0.040% ^{247}Cm, and 96.639% ^{248}Cm. Several pieces of the arc-shaped targets were mounted on a rotating wheel 100 mm in diameter which has eight sectors to mount the target pieces. Five pieces of the Cm target were used in most of the experiment, whereas six target pieces were used in a part of the experiment. On the sectors without Cm target, Ti foils of 0.91 mg/cm^2 thickness were mounted. For cooling the targets, the wheel was rotated at 1000 rpm during irradiation, and a beam was chopped electronically to not hit the target frame.

Rf isotopes were produced in bombardments of the Cm target with an ^{18}O beam. The ^{18}O beam was supplied from RILAC. Beam energies in laboratory frame were 88.2, 90.2, 94.8, and 101.3 MeV at the center of the target. The energy loss of the ^{18}O beam in the target was estimated to be 0.4 MeV at each beam energy. These energies were selected to be $\sigma_{4n} > \sigma_{5n}$ at 88.2 MeV, $\sigma_{4n} \approx \sigma_{5n}$ at 90.2 MeV, and $\sigma_{4n} \ll \sigma_{5n}$ at 101.3 MeV, where σ_{4n} and σ_{5n} are the production cross sections of $4n$ and $5n$ evaporation channels, respectively, based on the calculated production cross sections with the HIVAP code by Nishio *et al.* [24,25]. The beam intensity was monitored by 45° elastically scattered beam particles with a Si PIN (Positive-Intrinsic-Negative) photodiode (Hamamatsu S1223) 1.42 m downstream from the target position. The effective area of the photodiode was 3.6 × 3.6 mm^2. The typical beam intensity was 6 particle μA.

GARIS was used to separate the evaporation residues (ERs) in flight from the incident particles and the majority of by-products. GARIS was filled with He gas at a pressure of 33 Pa. Judging from the results of the previous experiments of ^{261}Rf production [21,26], a magnetic rigidity of GARIS was set at 1.73 T m. ERs recoiling out of the target were transported to the focal plane of GARIS where a Si semiconductor detector box was set.

The focal plane Si detector box was composed of a position-sensitive Si strip detector (PSD, Canberra PF-16CT-58*58-300EB) and four side Si semiconductor detectors (SSDs). ERs passing through GARIS were implanted in the PSD. The PSD is composed of 16 strips 3.63 mm wide and the effective area as a total is 58 × 58 mm^2. Each strip is position sensitive in the vertical direction, and the position resolution was 1 mm (FWHM). Each of the side SSD is composed of four Si PIN photodiodes (Hamamatsu S3584) with the effective area of 28 × 28 mm^2. The SSDs were used to measure α particles and SF fragments emitted backward from the PSD. Energy calibration of the PSD and SSDs was mainly performed by the major α line of ^{254}Fm (E_α = 7.192 MeV [12]) produced by transfer reactions. In part of the experiment, ^{210}Fr ($E_\alpha = 6.543$ MeV [12]) produced via the ^{197}Au(^{18}O,5n)^{210}Fr reaction was adopted for this purpose. The energy resolution for α particles observed in the PSD was 0.04 MeV (FWHM), whereas that observed in the SSD (and partially in the PSD) was 0.14 MeV. The detection efficiency of the PSD for the α particles emitted by ERs implanted in the PSD was 50% and that of the SSDs was 30%. One of the strip detectors was not used in part of measurements because an excessive amount of noise signals were observed. Therefore, the detection efficiency of the PSD for α particles became 47% in these measurements.

A beam on-off method was applied to measure decay events of Rf isotopes under low background conditions; that is, the beam was periodically switched on-off using a beam chopping system [27], and measurements were performed only in the beam off period. To distinguish a few-second SF activity and short-lived ^{262}Rf, the beam on-off periods at each beam energy were set to 6 s, 6 s and 0.1 s, 0.1 s. After irradiation at each beam energy, background events were measured for several hours to estimate the contribution from long-lived background SF events observed in the beam on-off measurements.

III. RESULTS

A. α-decay events

The observed α-particle spectra measured in the PSD and the SSDs at the ^{18}O beam energy of 94.8 MeV are shown in Fig. 1 as a typical example. In order to avoid unwanted implantation events of scattered beam particles due to inadequate beam chopping, the events occurred within 5 ms from the beginning of beam off periods were omitted from the analysis. At the beam energy of 94.8 MeV, the beam dose of 5.80 × 10^{17} and 7.25 × 10^{17} were accumulated in 6 s, 6 s and 0.1 s, 0.1 s measurements, respectively. In both measurements, the characteristic α lines of ^{261}Rf^{a} ($E_\alpha = 8.28$ MeV [7]) and its α-decay daughter nuclide ^{257}No ($T_{1/2} = 24.5$ s, $E_\alpha = 8.222$, 8.323 MeV [28]) were observed under low background conditions. The α events of these nuclides were almost equally distributed among all the strips of the PSD, indicating the proper magnetic field of GARIS for ^{261}Rf. On the other hand, the distribution of α events from transfer products was skew. Several α lines of nuclides produced by the transfer reactions such as Fm and Es isotopes were observed at $E_\alpha < 7.5$ MeV, whereas no remarkable α lines except for those from nuclides of interest were observed at $E_\alpha \geqslant 7.5$ MeV. In addition to the α lines of ^{261}Rf^{a} and ^{257}No, a small peak could be recognized at around 8.5 MeV as shown in Fig. 1(b). This energy corresponds to the reported α-particle energy of ^{261}Rf^{b} [17–21]. As described in Ref. [21], ^{212}Po^{m}

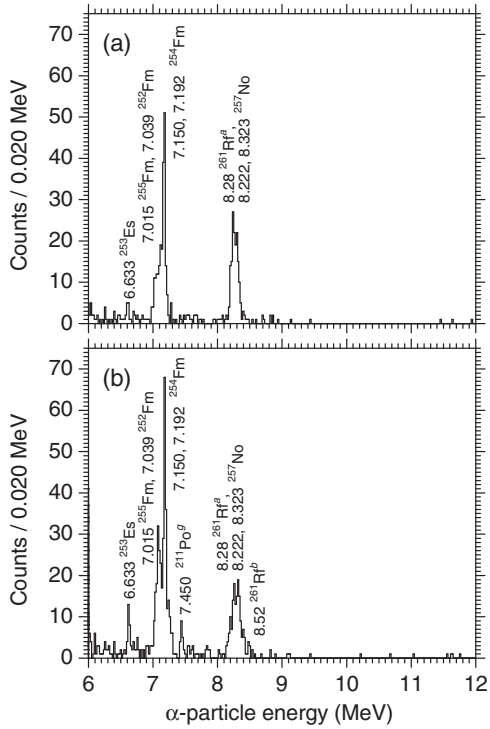

FIG. 1. Measured α-particle spectra in the PSD and SSDs at the ^{18}O beam energy of 94.8 MeV: (a) 6 s, 6 s measurement with the beam dose of 5.80×10^{17} and (b) 0.1 s, 0.1 s measurement with the beam dose of 7.25×10^{17}.

($T_{1/2} = 45.1$ s) emits α particle of 8.520 MeV with an intensity of 2.05% [12], which may cause unwanted background in the measurement of ^{261}Rf^{b}. Because α particles of ^{212}Po^{m} at 11.650 MeV with the highest intensity of 97% [12] were scarcely observed, the contribution of ^{212}Po^{m} at 8.520 MeV was regarded to be negligibly small. Similar α-particle spectra were obtained in other bombarding energies than 94.8 MeV.

The number of α events observed in the region of 8.00–8.42 MeV for ^{261}Rf^{a} and ^{257}No and 8.42–8.62 MeV for ^{261}Rf^{b} are listed in Table I. Due to the longer half-life of ^{261}Rf^{a} with respect to beam on-off periods, counting rates of α particles in 8.00–8.42 MeV for 6 s, 6 s measurements and 0.1 s, 0.1 s measurements were almost equal at the same bombarding energy. Most of the α events of 8.00–8.42 MeV were observed at the bombarding energy of 94.8 MeV, as expected from the excitation function of ^{248}Cm(^{18}O,5n)^{261}Rf^{a} [29].

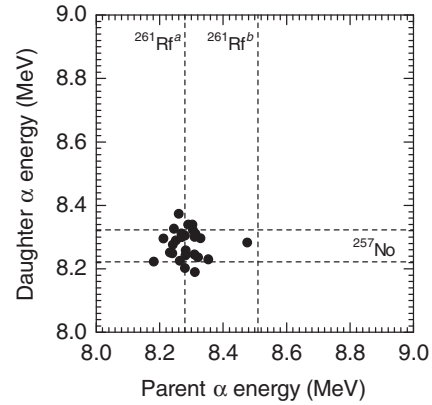

FIG. 2. Two-dimensional representation of time- and position-correlated α-α sequences observed in the PSD. The position window was set to ± 2 mm in the same strip, and the time window was set to 250 s. Dashed lines indicate the reported α-particle energies of ^{261}Rf^{a} ($E_\alpha = 8.28$ MeV [7]) and ^{261}Rf^{b} ($E_\alpha = 8.51$ MeV [20]) for parent α energy and that of ^{257}No ($E_\alpha = 8.222$, 8.323 MeV [28]) for daughter α energy.

We searched for α-α correlation events registered only in the PSD to reveal the genetic relationship between parent and daughter nuclei. In the whole experiment, we found 26 α-α correlation events with the position window of ± 2 mm in the same strip, time window of 250 s which correspond to 10 half-lives of ^{257}No, and α-particle energy range of $8.00 \leqslant E_\alpha \leqslant 10.00$ MeV. The results are summarized in Table I. Two-dimensional representation of the observed α-α sequences is shown in Fig. 2. Since the position resolution of the α particles measured in both of the PSD and the SSD is poor [23], we did not include the α events in the SSDs in correlation analysis. The difference of observed position between parent and daughter α particles of these 26 correlations were within 0.7 mm.

Almost all of the correlation events (25 events) were observed with a parent α energy ($E_{\alpha 1}$) range of 8.18–8.36 MeV and a daughter α energy ($E_{\alpha 2}$) range of 8.19–8.37 MeV. The average value of $E_{\alpha 1}$ was 8.28 ± 0.04 MeV, and

TABLE I. Summary of observed decay events.

Beam energy (MeV)	Beam on-off period (s)	Beam dose ($\times 10^{17}$)	α-decay events				SF events	Estimated background of SF events[a]
			$E_{\alpha 1} = 8.00$–8.42 MeV		$E_{\alpha 1} = 8.42$–8.62 MeV			
			α	α-α	α	α-α		
88.2	6	2.74	0	0	0	0	2	0.2 ± 0.1
88.2	0.1	12.61	7	0	1	0	45	22.6 ± 9.9
90.2	6	4.80	12	1	1	1	21	12.2 ± 5.7
90.2	0.1	3.32	6	0	0	0	18	8.7 ± 4.0
94.8	6	5.80	87	10	1	0	50	12.7 ± 6.3
94.8	0.1	7.25	93	10	6	0	58	17.4 ± 5.3
101.3	6	7.09	35	3	2	0	20	18.7 ± 9.5
101.3	0.1	4.55	18	1	0	0	25	14.9 ± 6.0

[a]Most of the background events resulted from ^{256}Fm.

half-life of daughter nuclide deduced from the average decay time was 19^{+5}_{-3} s (68% confidence interval). Hereafter, all errors adopted in this work correspond to a 68% confidence interval. The average value of $E_{\alpha 1}$ accords with that of ^{261}Rf^{a} ($E_\alpha = 8.28 \pm 0.02$ MeV [7,12]), and decay properties of the daughter nuclide agree with those of ^{257}No ($E_\alpha = 8.222$, 8.323 MeV, $T_{1/2} = 24.5 \pm 0.5$ s [28]). These 25 events are hence attributed to well-known α-α chains of ^{261}Rf^{a} and ^{257}No as expected [7,21,30]. The number of ^{261}Rf^{a}–^{257}No correlation events expected from α-singles events in the $E_{\alpha 1}$ range of 8.00–8.42 MeV (258 events) is 29 $\pm$ 2 taking into consideration the counting efficiency of the PSD and measurement time of beam on-off method. The observed number of correlation events is consistent with that expected.

It is noteworthy that one additional time- and position-correlated event with $E_{\alpha 1} = 8.48$ MeV and $E_{\alpha 2} = 8.28$ MeV was observed at the beam energy of 90.2 MeV. As mentioned in the context of α-particle spectra, the $E_{\alpha 1}$ of this correlation event coincides with the reported α-particle energy of ^{261}Rf^{b}. The $E_{\alpha 2}$ of this correlation, that is, the α energy of the daughter nuclide was in the same range with other 25 correlation events. The lifetime of daughter nuclide of this correlation event was 11.8 s. It is consistent with the half-life of ^{257}No. The estimated number of random α-α sequences in the energy region of 8.00–8.62 MeV was 0.14 for the whole experiment, indicating all the observed α-α correlation events were true ones. Therefore, the result of the search for α-α correlation events strongly supports the fact that ^{261}Rf^{b} emits the α particle of 8.51 MeV as reported so far [14,17–21].

We also searched for time- and position-correlated α-SF sequences in the parent α energy range of $8.00 \leqslant E_{\alpha 1} \leqslant 10.00$ MeV. No correlations were found within the position window of $\pm$2 mm in the same strip and time window of 250 s. A number of random α-SF sequences were estimated to be 0.091.

B. SF events

We regarded the coincidence events observed in the PSD with the energy greater than 30 MeV and in the SSD with the energy greater than 10 MeV as SF events. The observed SF events at each condition are summarized in Table I.

Background measurements were performed for longer than 15 h after irradiation at 90.2 and 94.8 MeV, and a SF activity with the half-life of 5.6 $\pm$ 4.3 h was observed. This activity could be attributed to one of the transfer products, ^{256}Fm ($T_{1/2} = 2.627$ h, $b_{\mathrm{SF}} = 0.919$ [12]) [8,31]. In addition to the decay component of 5.6 h half-life, almost constant component of SF activity was recognized at the rate of 0.054 ± 0.031 cph. Probably this longer component originated in the spattered fraction of the radioactive Cm target, judging from the fact that the α lines of ^{246}Cm were observed at around 5.4 MeV. After irradiation at 88.2 and 101.3 MeV, background measurements were performed for several hours. Several SF events were observed in these measurements. The number of background SF (^{256}Fm and long-lived component) events expected to be measured in the beam off period were estimated by standard growth and decay equations. The deduced number of background SF events for each run are listed at the last column in Table I.

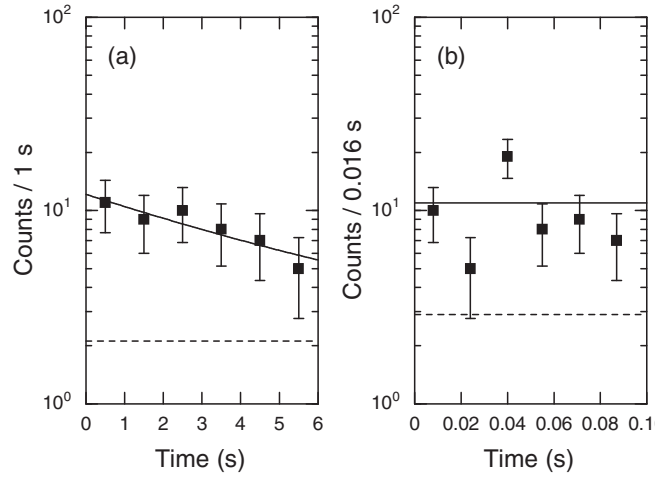

FIG. 3. SF events observed at the beam energy of 94.8 MeV. Dashed lines show the number of estimated background (mainly ^{256}Fm). (a) 6 s, 6 s measurement. Solid line indicates the decay curve of observed SF events considering the background events denoted by dashed line. (b) 0.1 s, 0.1 s measurement. Solid line indicates the sum of the contribution of the 1.9-s SF events and the estimated background events.

Observed SF events at the beam energy of 94.8 MeV were shown in Fig. 3 as a function of time from the beginning of the beam off period. At this energy, 50 and 58 events were observed in 6 s, 6 s measurement and 0.1 s, 0.1 s measurement, respectively. In the 6 s, 6 s measurement, a decay component of SF events was clearly seen, as shown in Fig. 3(a). The half-life of this component was evaluated to be 3.9 $\pm$ 3.0 s, taking into account a long-lived SF background component (mainly ^{256}Fm) as indicated by a dashed line in the figure. The deduced half-life of 3.9 ± 3.0 s was consistent with that of the previously reported half-lives of the SF nuclides assigned to ^{261}Rf^{b} and ^{262}Rf (1.2–4.7 s). This component may be ^{259}Fm as reported in Ref. [8]. However, this possibility could be excluded by a following consideration. From the systematics of production cross sections of $^{252-256}$Fm as transfer products in ^{248}Cm + ^{18}O reaction [31], cross section of ^{259}Fm at the beam energy of about 97 MeV was estimated to be approximately 3 nb. The expected number of SF events of ^{259}Fm was approximately 0.01, which was estimated from the production cross-section ratio of ^{259}Fm and ^{254}Fm and the observed α events of ^{254}Fm. The estimated value, 0.01, is negligibly small compared with the observed one, 50. For the half-life of this component, the reported most precise one is 1.9 $\pm$ 0.4 s, which was obtained under an extremely low background condition [21]. Hereafter, we adopt 1.9 s for the half-life of this component.

In 6 s, 6 s measurement at 94.8 MeV, the α and SF branches for 1.9-s SF nuclide were determined to be $b_\alpha = 0.12 \pm 0.05$ and $b_{\mathrm{SF}} = 0.88 \pm 0.05$, respectively. The b_α value of this work agrees with that reported for ^{261}Rf^{b} as a granddaughter nuclide of ^{269}Hs ($b_\alpha = 0.09$ [18]) and as a daughter nuclide of ^{265}Sg^{a,b} ($b_\alpha = 0.18 \pm 0.09$ [20]; the superscripts a and b denote two isomeric states in ^{265}Sg), whereas it is slightly smaller than that

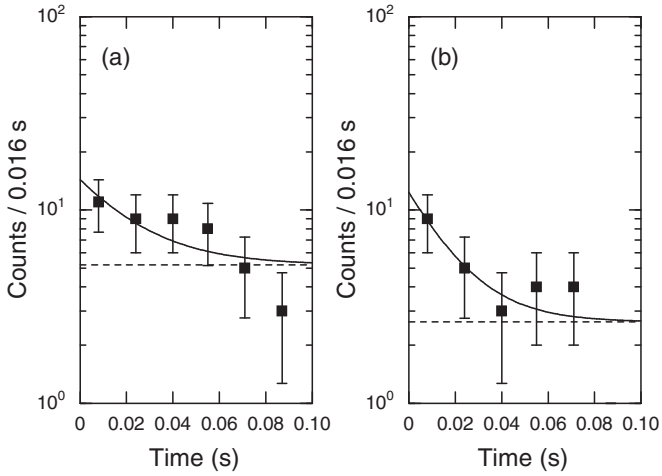

FIG. 4. Short-lived SF components observed in 0.1 s, 0.1 s measurements. Dashed lines show the sum of the estimated background events and the contribution of the 1.9-s SF events. Solid lines show the decay curves of short-lived components considering the background events denoted by dashed lines. (a) SF events observed at 88.2 MeV. (b) SF events observed at 101.3 MeV.

observed by direct production of ^{261}Rf^{b} by the ^{248}Cm(^{18}O,5n) reaction ($b_\alpha = 0.27 \pm 0.06$ [21]).

No short-lived component of SF decay was observed in 0.1 s, 0.1 s measurement as shown in Fig. 3(b). Note that the 1.9-s SF component observed in the 6 s, 6 s measurement behaves as a long-lived component in the 0.1 s, 0.1 s measurement. The observed number of SF events was consistent with the sum of the estimated number of background and the contribution of the 1.9-s component, which means that the cross section of ^{262}Rf ($T_{1/2} = 47$ ms [9]) is very small at the beam energy of 94.8 MeV. The short-lived SF activity was not recognized at the beam energy of 94.8 MeV, whereas the short-lived components were clearly seen at 88.2 and 101.3 MeV as shown in Fig. 4. The half-lives were evaluated to be 17 ± 16 ms and 12 ± 11 ms for those components observed at 88.2 and 101.3 MeV, respectively, taking into account the background and the contribution of the 1.9-s SF components observed in 6 s, 6 s measurements as the same manner with Fig. 3(a). The large errors in half-lives were due to a large number of background events and inadequate counting statistics. At least, however, the short-lived SF activities were clearly recognized at 88.2 and 101.3 MeV.

IV. DISCUSSION

A. Excitation function of ^{248}Cm(^{18}O,5n)^{261}Rf$^{\alpha}$

Only α-decay mode was reported on the disintegration for both ^{261}Rf$^{\alpha}$ and ^{257}No. Kadkhodayan *et al.* [22] estimated an upper limit of 0.11 for $b_{\rm SF}$ of ^{261}Rf$^{\alpha}$ observed by a gas chromatographic separation method of $RfCl_4$. Haba *et al.* [21] derived a similar upper limit of 0.13 for $b_{\rm SF}$ of ^{261}Rf$^{\alpha}$ measured using a gas-jet transport system connected with GARIS. As to ^{257}No, the upper limit of 0.073 for $b_{\rm SF}$ was derived from the result of correlation event search (26 α-α correlations and no α-SF correlation). Lazarev *et al.* [30] calculated an upper limit of 0.015 for $b_{\rm SF}$ based on the total number of the α particles of ^{261}Rf$^{\alpha}$ and ^{257}No, the number of the correlated α-α events, and the undetected α-SF correlation event. As no positive results for the SF branch of ^{261}Rf$^{\alpha}$ and ^{257}No were reported, we assumed an α branch (b_α) of unity for both ^{261}Rf$^{\alpha}$ and ^{257}No in the following consideration.

At the ^{18}O beam energy of 94.8 MeV, the transport efficiency of GARIS was evaluated to be 4.7 ± 1.2% for the PSD area (58 × 58 mm^2), assuming the production cross section at this beam energy is 12 ± 3 nb [21,29]. Since the distribution of ERs at the focal plane by multiple scatterings by target and He atoms depends on the recoil energy of ERs, the yield of ERs at the focal plane of GARIS depends slightly on the ^{18}O beam energy. For example, the relative transport efficiencies against that of 94.8 MeV were estimated to be 0.86, 0.90, and 1.1 at the beam energies of 88.2, 90.2, and 101.3 MeV, respectively, assuming ^{238}U as a recoil atom and as a target nucleus using the TRIM program [32], as described in Ref. [33]. As a result, the actual cross sections at 88.2 and 90.2 MeV would be slightly higher than the observed ones and slightly lower at 101.3 MeV. However, the accurate estimation of the energy dependence of the transmission efficiency is difficult and the trans-uranium nuclei are not adopted in the commonly used simulation programs such as TRIM [32]. Therefore, in this work, the energy dependence of the transmission efficiency was not included in the evaluation of cross sections.

The production cross sections of ^{261}Rf$^{\alpha}$ were evaluated from the observed number of α particles in the energy range of 8.00–8.42 MeV. The obtained values were 0.47 ± 0.20, 1.8 ± 0.6, 12 ± 3, and 4.1 ± 1.1 nb at the ^{18}O incident energies of 88.2, 90.2, 94.8, and 101.3 MeV, respectively. The contribution from directly produced ^{257}No in the reaction of ^{248}Cm(^{18}O,α5n)^{257}No is negligible in the studied energy region [3,29]. The obtained excitation function is shown in Fig. 5(a) together with the reported production cross sections of ^{261}Rf$^{\alpha}$ [7,29,34], where the relative cross sections reported by Silva *et al.* [34] are normalized to the data of Nagame *et al.* [29]. Cross section of the ^{248}Cm(^{18}O,5n)^{261}Rf$^{\alpha}$ reaction exhibits the maximum at 94.8 MeV, and the shape of the excitation function is in good agreement with those reported previously.

B. Excitation functions for production of SF nuclides

The production cross sections of the SF nuclide with the 1.9-s half-life were derived by comparison with the yield of ^{261}Rf$^{\alpha}$. The yield of the 8.51-MeV α particle was also included in the cross section of the SF nuclide. Although 1.9-s SF decay was not observed clearly at the ^{18}O energies other than 94.8 MeV, the 1.9-s SF component was deduced from the difference between the observed number of SF events and estimated number of long-lived background SF events in 6 s, 6 s measurements at each beam energy. The production cross sections of 1.9-s SF nuclide were evaluated to be $1.5^{+1.8}_{-1.5}$, 3.7± 3.0, 12 ± 4, and $0.9^{+2.6}_{-0.9}$ nb at the ^{18}O incident energies of 88.2, 90.2, 94.8, and 101.3 MeV, respectively. The excitation function of this nuclide is shown in Fig. 5(b) together with the available cross-sectional data reported in Ref. [21].

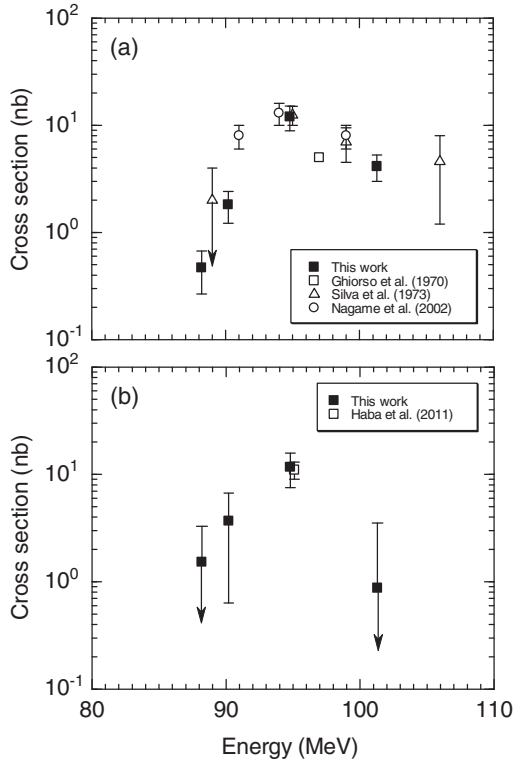

FIG. 5. Excitation functions for the production of ^{261}Rf^{a} and 1.9-s SF nuclide in ^{248}Cm + ^{18}O reaction. Beam energies are represented in laboratory frame. (a) Excitation function of the ^{248}Cm(^{18}O,5n)^{261}Rf^{a} reaction. The data of the production cross section of ^{261}Rf^{a} from the Refs. [7,29,34] are also shown as open symbols. (b) Excitation function for the production of the 1.9-s SF nuclide. Cross sections were evaluated from the 1.9-s SF component and the 8.51-MeV α branch. The production cross section from Ref. [21] is also shown.

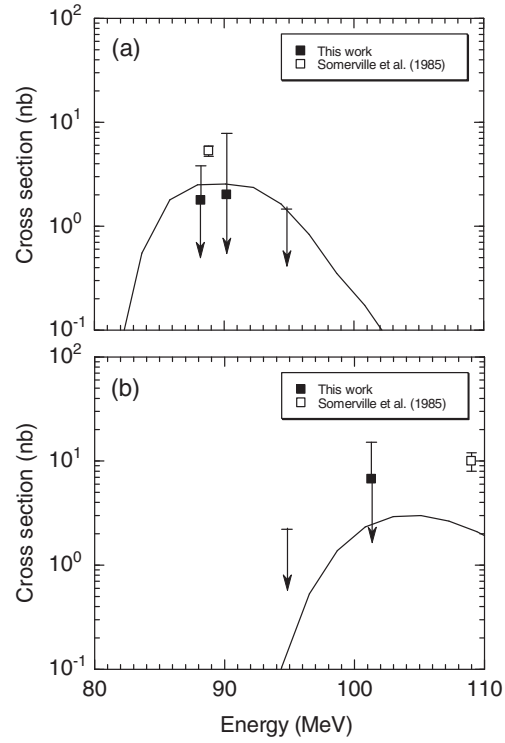

FIG. 6. Excitation functions for the production of short-lived SF nuclides observed in 0.1, s 0.1 s measurements. Beam energies are represented in the laboratory frame. The arrows denote the upper limits evaluated in this work. Solid lines indicate the HIVAP prediction calcurated by Nishio *et al.* [24,25]. The available cross-sectional data in Ref. [9] are also shown. (a) Excitation function for the production of ^{262}Rf via 4n evaporation channel. (b) Excitation function for the production of ^{260}Rf via 6n evaporation channel.

The resulting excitation function exhibits the maximum cross section of 12 ± 4 nb at 94.8 MeV. This value agrees well with that reported by Haba *et al.* [21]. The shape of this excitation function is very similar to that of ^{261}Rf^{a} shown in Fig. 5(a), indicating that 1.9-s SF nuclide is surely ^{261}Rf^{b} which is the isomer of ^{261}Rf^{a}.

The short-lived SF activities were recognized at the beam energies of 88.2 MeV with the half-life of 17 ± 16 ms and 101.3 MeV with the half-life of 12 ± 11 ms. If these SF activities originated from the same nuclide, the same activity must be observed at the beam energy between 88.2 and 101.3 MeV. Because such a short-lived component was not observed at the beam energy of 94.8 MeV, each of these components was considered to originate from different nuclides. Judging from the observed beam energies and half-lives, these components observed at 88.2 and 101.3 MeV were assigned to ^{262}Rf ($T_{1/2}$ = 47 ms [9,12]) and ^{260}Rf ($T_{1/2}$ = 20.1 ms [12]), respectively. Since the large errors were attached for the half-lives of these nuclides, we adopted the reported values of half-lives (47 ms for ^{262}Rf and 20.1 ms for ^{260}Rf) for data analysis.

The excitation functions for the production of ^{262}Rf and ^{260}Rf observed in the 0.1 s, 0.1 s measurements were evaluated in order to compare with that of the 1.9-s SF nuclide. Although a short-lived SF decay component was not clearly seen at 90.2 MeV, the number of SF events of ^{262}Rf was deduced from the difference between the observed number of SF events and sum of estimated number of long-lived background SF events and contribution of 1.9-s SF component observed in the 6 s, 6 s measurement. The production cross sections of ^{262}Rf were evaluated to be $1.8^{+2.0}_{-1.8}$ nb for the ^{18}O beam energy of 88.2 MeV and $2.0^{+5.8}_{-2.0}$ nb at 90.2 MeV. At 101.3 MeV, the production cross section of ^{260}Rf was evaluated to be $6.7^{+8.4}_{-6.7}$ nb. At 94.8 MeV, upper limits of the production cross sections for 4n and 6n channels were evaluated to be 1.5 and 2.2 nb, respectively. The resulting excitation functions for the production of ^{262}Rf and ^{260}Rf are shown in Fig. 6 together with the available cross-sectional data [9] and the HIVAP prediction calculated by Nishio *et al.* [24,25]. The shapes of the excitation functions of the ^{248}Cm(^{18}O,4n)^{262}Rf and ^{248}Cm(^{18}O,6n)^{260}Rf reactions are consistent with the reported data by Somerville *et al.* [9] and the HIVAP prediction [24,25]. The shape of these excitation functions are clearly different from that of 1.9-s SF nuclide. Therefore, we concluded that the nuclide with 1.9-s SF decay should be assigned to ^{261}Rf^{b}.

The half-life of 17 ± 16 ms evaluated for ^{262}Rf in this work is shorter than that reported by Somerville *et al.* (47 ± 5 ms

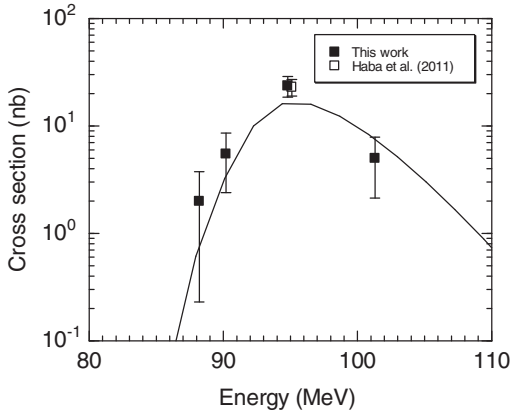

FIG. 7. Excitation function for the production of ^{261}Rf via 5n evaporation channel evaluated from sum of the cross sections of ^{261}Rf^{a} [Fig. 5(a)] and the 1.9-s SF nuclide identified as ^{261}Rf^{b} in this work [Fig. 5(b)]. The available cross-sectional data in Ref. [21] is also shown.

[9]). On the other hand, Gorshkov *et al.* [35] reported that they observed much longer half-life of 210^{+128}_{-58} ms for ^{262}Rf produced in the reaction of ^{244}Pu + ^{22}Ne. Since long-lived SF nuclides such as ^{256}Fm were accumulated in the detector during irradiation, we could not observe such a component. It is necessary to reduce background SF events to deduce the half-life of ^{262}Rf more exactly.

The total cross sections of ^{261}Rf which are the sum of the production cross sections of ^{261}Rf^{a} and ^{261}Rf^{b} were evaluated to be 2.0 ± 1.8, 5.5 ± 3.1, 24 ± 5, and 5.0 ± 2.9 nb at the ^{18}O beam energies of 88.2, 90.2, 94.8, and 101.3 MeV, respectively. The resulting excitation function of ^{261}Rf is shown in Fig. 7 together with the cross section reported in Ref. [21] and the HIVAP prediction [24,25]. The production cross section of ^{261}Rf $\sigma(^{261}\mathrm{Rf}^{a} + {}^{261}\mathrm{Rf}^{b}) = 24 \pm 5$ nb and the ratio of the cross sections $\sigma(^{261}\mathrm{Rf}^{a})/\sigma(^{261}\mathrm{Rf}^{b}) = 1.0 \pm 0.5$ at 94.8 MeV are in good agreement with those reported by Haba *et al.* (23 ± 4 nb and 1.1 ± 0.2 at 95.1 MeV [21]). The shape of excitation function of ^{261}Rf is also similar with that predicted by the HIVAP calculation [24,25].

In this work, a 8.51-MeV α branch in ^{261}Rf^{b} was clearly recognized by α-α correlation search. The time- and position-correlated α-α sequences observed in the reaction of ^{244}Pu + ^{22}Ne with similar methods were reported by Lazarev *et al.* [30]. Although they reported 69 correlations, no correlations were observed in the $E_{\alpha 1}$ range of 8.42–8.62 MeV. Further, the cross-sectional ratio of $\sigma(^{261}\mathrm{Rf}^{a})/\sigma(^{261}\mathrm{Rf}^{b})$ is reported to be ∼2.5 in ^{244}Pu + ^{22}Ne reaction [35]. It seems that the cross-sectional ratio $[\sigma(^{261}\mathrm{Rf}^{a})/\sigma(^{261}\mathrm{Rf}^{b})]$ considerably depends on the reaction system.

V. CONCLUSION

The excitation functions for the production of Rf isotopes in ^{248}Cm + ^{18}O reaction were measured at the focal plane of GARIS. The ^{18}O beam energies of 88.2, 90.2, 94.8, and 101.3 MeV were used. Using a beam on-off method, the characteristic α lines of ^{261}Rf^{a} and daughter nuclide ^{257}No were observed under low background conditions. In addition to the α-α correlations of ^{261}Rf^{a} and ^{257}No, one α-α correlation event of the nuclide assigned to ^{261}Rf^{b} and ^{257}No was observed. The excitation function of the ^{248}Cm(^{18}O,5n)^{261}Rf^{a} reaction exhibited the maximum cross section at 94.8 MeV, and it was in good agreement with reported ones. At 94.8 MeV, a SF activity with the half-life of 3.9 ± 3.0 s was observed. The excitation function of this component exhibited a similar shape to that of ^{261}Rf^{a}. This result strongly supports that the SF nuclide is ^{261}Rf^{b}. Furthermore, short-lived SF components with the half-lives of 17 ± 16 ms and 12 ± 11 ms were observed at the beam energies of 88.2 and 101.3 MeV, respectively. Since such the short-lived components were not observed at 94.8 MeV, each of these components was considered to originate from different nuclides. Judging from the observed beam energies and half-lives, we assigned these nuclides observed in 88.2 and 101.3 MeV to ^{262}Rf and ^{260}Rf, respectively. The excitation functions of the ^{248}Cm(^{18}O,4n)^{262}Rf and ^{248}Cm(^{18}O,6n)^{260}Rf reactions were clearly different from that tentatively assigned to ^{261}Rf^{b}. Therefore, we conclude that a few-second SF nuclide previously assigned to both ^{261}Rf^{b} and ^{262}Rf is not ^{262}Rf but ^{261}Rf^{b}. The excitation functions of ^{260}Rf, ^{261}Rf, and ^{262}Rf were consistent with those of the HIVAP prediction.

ACKNOWLEDGMENTS

This work was performed at the RI Beam Factory operated by RIKEN Nishina Center and CNS, University of Tokyo. The authors are grateful to the crew of the RIKEN Heavy-Ion Linear Accelerator for providing the intense beam. The authors also thank K. Nishio of Japan Atomic Energy Agency for providing the data of the HIVAP prediction. This research was partially supported by a Grant-in-Aid for Specially Promoted Research No. 19002005, from the Ministry of Education, Culture, Sports, Science, and Technology, Japan.

[1] M. Schädel, Angew. Chem. Int. Ed. **45**, 368 (2006).
[2] M. Schädel, Acta Phys. Pol. B **34**, 1701 (2003).
[3] Y. Nagame, J. Nucl. Radiochem. Sci. **6**, A21 (2005).
[4] J. V. Kratz, Radiochim. Acta **99**, 477 (2011).
[5] A. Türler and V. Pershina, Chem. Rev. **113**, 1237 (2013).
[6] M. Asai (private communication).
[7] A. Ghiorso, M. Nurmia, K. Eskola, and P. Eskola, Phys. Lett. B **32**, 95 (1970).
[8] D. C. Hoffman, D. Lee, A. Ghiorso, M. J. Nurmia, K. Aleklett, and M. Leino, Phys. Rev. C **24**, 495 (1981).
[9] L. P. Somerville, M. J. Nurmia, J. M. Nitschke, A. Ghiorso, E. K. Hulet, and R. W. Lougheed, Phys. Rev. C **31**, 1801 (1985).
[10] Y. A. Lazarev, Y. V. Lobanov, Y. T. Oganessian, V. K. Utyonkov, F. S. Abdullin, G. V. Buklanov, B. N. Gikal, S. Iliev, A. N. Mezentsev, A. N. Polyakov *et al.*, Phys. Rev. Lett. **73**, 624 (1994).

[11] M. R. Lane, K. E. Gregorich, D. M. Lee, M. F. Moher, M. Hsu, C. D. Kacher, B. Kadkhodayan, M. P. Neu, N. J. Stoyer, E. R. Sylwester *et al.*, Phys. Rev. C **53**, 2893 (1996).
[12] R. B. Firestone and V. S. Shirley, eds., *Table of Isotopes*, 8th ed. (John Wiley & Sons, New York, 1996).
[13] S. Hofmann, V. Ninov, F. P. H. Berger, P. Armbruster, H. Folger, G. Münzenberg, H. J. Schött, A. G. Popeko, A. V. Yeremin, S. Saro *et al.*, Z. Phys. A **354**, 229 (1996).
[14] S. Hofmann, F. P. Heßberger, D. Ackermann, G. Münzenberg, S. Antalic, P. Cagarda, B. Kindler, J. Kojouharova, M. Leino, B. Lommel *et al.*, Eur. Phys. J. A **14**, 147 (2002).
[15] K. Morita, K. Morimoto, D. Kaji, T. Akiyama, S. Goto, H. Haba, E. Ideguchi, K. Katori, H. Koura, H. Kudo *et al.*, J. Phys. Soc. Jpn. **76**, 043201 (2007).
[16] T. Sumita, K. Morimoto, D. Kaji, H. Haba, K. Ozeki, R. Sakai, A. Yoneda, A. Yoshida, H. Hasebe, K. Katori *et al.*, J. Phys. Soc. Jpn. **82**, 024202 (2013).
[17] J. Dvorak, W. Brüchle, M. Chelnokov, R. Dressler, C. E. Düllmann, K. Eberhardt, V. Gorshkov, E. Jäger, R. Krücken, A. Kuznetsov *et al.*, Phys. Rev. Lett. **97**, 242501 (2006).
[18] J. Dvorak, W. Brüchle, M. Chelnokov, C. E. Düllmann, Z. Dvorakova, K. Eberhardt, E. Jäger, R. Krücken, A. Kuznetsov, Y. Nagame *et al.*, Phys. Rev. Lett. **100**, 132503 (2008).
[19] C. E. Düllmann and A. Türler, Phys. Rev. C **77**, 064320 (2008).
[20] H. Haba, D. Kaji, Y. Kudou, K. Morimoto, K. Morita, K. Ozeki, R. Sakai, T. Sumita, A. Yoneda, Y. Kasamatsu *et al.*, Phys. Rev. C **85**, 024611 (2012).
[21] H. Haba, D. Kaji, H. Kikunaga, Y. Kudou, K. Morimoto, K. Morita, K. Ozeki, T. Sumita, A. Yoneda, Y. Kasamatsu *et al.*, Phys. Rev. C **83**, 034602 (2011).
[22] B. Kadkhodayan, A. Türler, K. E. Gregorich, P. A. Baisden, K. R. Czerwinski, B. Eichler, H. W. Gäggeler, T. M. Hamilton, D. T. Jost, C. D. Kacher *et al.*, Radiochim. Acta **72**, 169 (1996).
[23] K. Morita, K. Morimoto, D. Kaji, H. Haba, K. Ozeki, Y. Kudou, N. Sato, T. Sumita, A. Yoneda, T. Ichikawa *et al.*, J. Phys. Soc. Jpn. **78**, 064201 (2009).
[24] K. Nishio, H. Ikezoe, Y. Nagame, M. Asai, K. Tsukada, S. Mitsuoka, K. Tsuruta, K. Satou, C. J. Lin, and T. Ohsawa, Phys. Rev. Lett. **93**, 162701 (2004).
[25] K. Nishio (private communication).
[26] H. Haba, D. Kaji, Y. Komori, Y. Kudou, K. Morimoto, K. Morita, K. Ooe, K. Ozeki, N. Sato, A. Shinohara *et al.*, Chem. Lett. **38**, 426 (2009).
[27] D. Kaji, K. Morimoto, A. Yoneda, H. Hasebe, A. Yoshida, H. Haba, S. Goto, H. Kudo, and K. Morita, Nucl. Instrum. Methods Phys. Res. A **590**, 198 (2008).
[28] M. Asai, K. Tsukada, M. Sakama, S. Ichikawa, T. Ishii, Y. Nagame, I. Nishinaka, K. Akiyama, A. Osa, Y. Oura *et al.*, Phys. Rev. Lett. **95**, 102502 (2005).
[29] Y. Nagame, M. Asai, H. Haba, S. Goto, K. Tsukada, I. Nishinaka, K. Nishio, S. Ichikawa, A. Toyoshima, K. Akiyama *et al.*, J. Nucl. Radiochem. Sci. **3**, 85 (2002).
[30] Y. A. Lazarev, Y. V. Lobanov, Y. T. Oganessian, V. K. Utyonkov, F. S. Abdullin, A. N. Polyakov, J. Rigol, I. V. Shirokovsky, Y. S. Tsyganov, S. Iliev *et al.*, Phys. Rev. C **62**, 064307 (2000).
[31] D. Lee, K. J. Moody, M. J. Nurmia, G. T. Seaborg, H. R. von Gunten, and D. C. Hoffman, Phys. Rev. C **27**, 2656 (1983).
[32] J. F. Ziegler, M. D. Ziegler, and J. P. Biersack, Nucl. Instrum. Methods Phys. Res. B **268**, 1818 (2010).
[33] D. Kaji, K. Morita, K. Morimoto, H. Haba, and H. Kudo, Proc. Radiochim. Acta **1**, 105 (2011).
[34] R. J. Silva, P. F. Dittner, M. L. Mallory, O. L. Keller, K. Eskola, P. Eskola, M. Nurmia, and A. Ghiorso, Nucl. Phys. A **216**, 97 (1973).
[35] A. Gorshkov, R. Graeger, A. Türler, A. Yakushev, D. Ackermann, W. Brüchle, C. E. Düllmann, E. Jäger, F. Heßberger, J. Khuyagbaatar *et al.*, GSI Sci. Rep. **2008**, 140 (2009).